

# Effect of Sectional Damage Model on Globe Damage Evolution of Concrete Structures



Y.L. Liu, Z. He\* & X.Y. Ou  
Dalian University of Technology, China

## SUMMARY:

Three damage models for reinforced concrete sections, i.e. the modified Park-Ang model, Bracci et al's model and the Roufaiel-Meyer model, are selected and critically reviewed through mathematical expression, applicability, etc. Incremental dynamic analysis (IDA) using the platform OpenSees is then performed to evaluate the position of initial failed section and corresponding spectral acceleration ( $S_a$ ), the number of subsequent failed sections and their positions, etc. More ground motions are introduced to carry out a parametric study, trying to find out the failure mode of maximum probability by principal component analysis (PCA) method in the mathematical statistics as  $S_a$  increases. The results show that the failure modes obtained by the three models under same ground motion are largely uniform. The discrete structural failure modes under different ground motions can be very well controlled based on normal design. It is feasible that the failure mode of maximum probability can be predicted by PCA.

*Keywords: sectional damage model, ground motion, failure mode, principal component analysis*

## 1. INSTRUCTIONS

Failure of structures caused by severe earthquake actions heavier load is primarily caused by their non-optimal failure modes (Bai & Ou, 2011). In the actual structural analysis, with the structural members and redundancy increasing, structural failure modes increase in the form of a series (Hou, 2001), such as super high-rise structures, large span structures, etc. It is not possible for current computational condition to find out all structural failure modes. The multiple structural failure modes under different ground motions make structural damage mechanism and collapse analysis extremely difficult. Therefore, how to find out the failure mode of maximum probability under different ground motions, and control it by enhancing the weakest structural member, having a very vital significance to calculate structural reliability and improve structural collapse resistant capacity.

In the past few decades, many methods to identify the main structural failure modes were proposed at home and abroad. According to the basis of discrimination and way of search, they can be divided into criteria method and rational analytical method. Criterion method depended on the element stress severity to search the key component in failure modes, it was first proposed by Moses (Moses, 1992), and used for analyzing truss structures. Feng (Feng, 1988) developed the optimal criteria method and the incremental load minimum criterion on that basis. Yao and Gu (Yao & Gu, 1996) improved the automatic matrix force method. Rational analysis method adopted the probability of failure as the index to identify structural failure modes, mainly including the following several kinds of methods, i.e., the branch-bound method (Murotsu et al, 1984), the truncate enumeration method (Melchers & Tang, 1984) and the  $\beta$ -bound method (Thoft-christensen & Murotsu, 1986), etc. However, both criteria method and rational analysis method cannot guarantee that the main failure mode is omitted. Recently, some new methods are proposed. Gharaibeh et al (Gharaibeh et al., 2002) proposed two important factors as member reliability and member post-failure, and used the factors to evaluate the key members of highway bridge and offshore platform. Park et al (Park et al, 2004) presented a method to

calculate complex structures based on the reliability of member or unit, and analyzed truss structural failure mode. From above it can be seen that all these methods do not well consider the variation caused by different ground motion on structural response, and lack of a statistically significant conclusion. Therefore, this is the focus study of the article.

Considering the universal application of reinforced concrete structures, a four-storey and three-bay reinforced concrete planar frame is established, three damage models for reinforced concrete sections are used to analyze structural failure modes, i.e. the modified Park-Ang model, Bracci et al's model and the Roufaiel-Meyer model, are selected and critically reviewed through mathematical expression, applicability, etc. Incremental dynamic analysis (IDA) using the platform OpenSees is then performed to evaluate the position of initial failed section and corresponding  $S_a$ , the number of subsequent failed sections and their positions, etc. More ground motions are introduced to carry out a parametric study, trying to find out the failure mode of maximum probability by principal component analysis (PCA) method in the mathematical statistics as  $S_a$  increases.

## 2. INTRODUCTION OF STRUCTURAL DAMAGE MODELS

Recently, many structural damage models for reinforced concrete members have been proposed, due to the influence factors of structural damage are more complicated, there are numerous variations among these damage models. In summary, they can be broadly divided into three categories as follows: deformation-based, energy-based, combination of deformation and energy. The damage analysis of structure or member under seismic load shows that the earthquake is a reciprocating action, and hold time is short, the damage of structure or member firstly shows the cumulative damage of cross-section. Therefore, three damage models for reinforced concrete sections, i.e. the modified Park-Ang model (Kunnath et al., 1992), Bracci et al's model (Bracci et al., 1985) and the Roufaiel-Meyer model (Roufaiel & Meyer, 1987), are selected and critically reviewed through mathematical expression, applicability, etc.

### 2.1 Modified Park-Ang Model

Kunnath et al (1992) proposed a modified version of the Park and Ang index (Park & Ang, 1985) and applied it into the original release of IDARC, in which the moment and curvature were used instead of force and displacement:

$$D = \frac{\phi_m - \phi_r}{\phi_u - \phi_r} + \beta \frac{\int dE}{M_y \phi_u} \quad (2.1)$$

In which,  $\phi_m$  is maximum record curvature under seismic load,  $\phi_r$  is the restoring curvature,  $\phi_u$  is the ultimate curvature capacity under monotonic loading,  $M_y$  is the yield moment of the section,  $\int dE$  is the total dissipated hysteretic energy (enclosed area of  $M-\phi$  loops),  $\beta$  is a non-negative parameter. Park, et al (Park et al., 1987) suggested the following detailed damage classification:  $D < 0.1$  indicates no damage-localised minor cracking;  $0.1 \leq D < 0.25$  indicates minor damage-light cracking throughout;  $0.25 \leq D < 0.4$  indicates moderate damage-severe cracking, localised spalling;  $0.4 \leq D < 1.0$  indicates severe damage-crushing of concrete, reinforcement exposed;  $D \geq 1.0$  indicates collapsed.

### 2.2 Bracci et al's Model

Bracci et al (1985) presented a further combined damage model. They defined the damage potential  $D_p$  as the total area between the monotonic load-deformation curve and the fatigue envelop in Fig. 2.1(a). As the evolution of the damage, the load-deformation curve degraded, resulting in strength damage  $D_s$ , and irrecoverable deformation occurred, causing deformation damage  $D_d$ . These damage parameters were given by the shaded areas shown in Fig. 2.1(a). Bracci et al (1985) used the simplified bilinear moment-curvature relationship shown in Fig. 2.1(b). The proportionate strength loss and proportionate

plastic deformation can then be defined as:

$$D_M = \frac{\Delta M}{M_y} \quad D_\phi = \frac{\phi_a - M_a / k_a}{\phi_u - M_u / k_u} \quad (2.2)$$

$$D = \frac{D_s + D_d}{D_p} = \frac{\Delta M(\phi_f - \phi_y) + (M_y - \Delta M)(\phi_m - \phi_y)}{M_y(\phi_f - \phi_y)} = D_M + D_\phi - D_M D_\phi \quad (2.3)$$

Bracci et al (1985) suggested a calculation method for  $D_\phi$  in which the value of yield curvature was modified after cycle, taking account of both plastic deformations and effect of stiffness degradation, as shown in Fig. 2.1(c). The strength degradation was calculated from:

$$\Delta M = \frac{c \int dE}{\phi_y} \quad (2.4)$$

In which, the constant  $c$  is defined by a regression equation in terms of the axial load, the longitudinal and confinement steel ratios, and the material strengths.

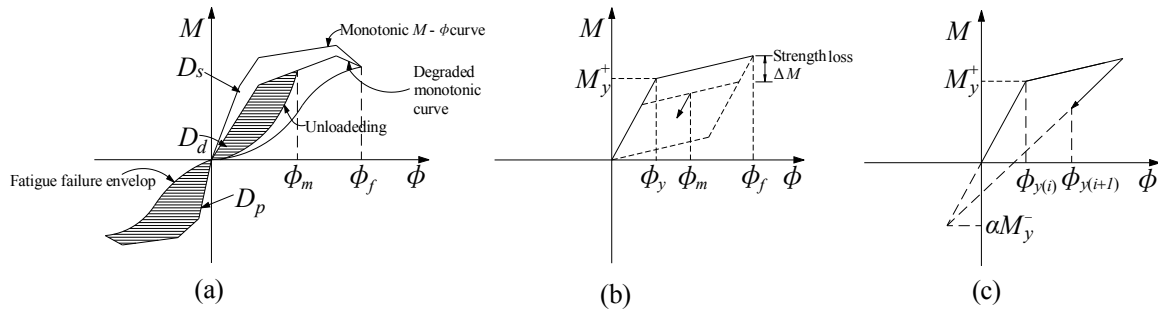


Figure 2.1. Moment-Curvature characteristic for index of Bracci et al

Bracci et al (1985) suggested the following correlation with damage states:  $D \leq 0.33$  represents a serviceable damage state;  $0.33 < D \leq 0.66$  represents a repairable damage state;  $0.66 < D \leq 1.0$  represents an irreparable damage state and  $D > 1.0$  represents a collapsed state.

### 2.3 Roufaiel-Meyer Model

Roufaiel and Meyer (1987) suggested a modified form of the flexural damage ratio based on the Banon et al's model (Banon et al, 1987) defined as the increase in flexibility between the initial condition and the instant of maximum deformation divided by the increase in flexibility at failure. This can be expressed as (see Fig. 2.2):

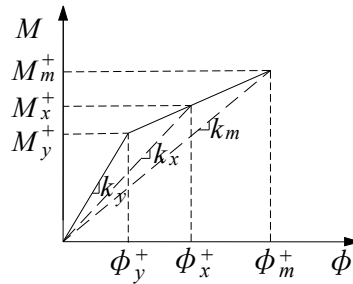


Figure 2.2. Definition of modified flexural damage ratio

$$D = \max(D^+, D^-) \quad (2.5)$$

Superscripts + and – denote loading direction. As defined by Roufaiel and Meyer in Ref. (Roufaiel & Meyer, 1987),  $D=0$  shows no damage in structural components and  $D=1.0$  indicates the onset of global structural failure.

$$\text{in which } D^+ = \frac{\frac{\phi_x^+}{M_x^+} - \frac{\phi_y^+}{M_y^+}}{\frac{\phi_m^+}{M_m^+} - \frac{\phi_y^+}{M_y^+}} \quad D^- = \frac{\frac{\phi_x^-}{M_x^-} - \frac{\phi_y^-}{M_y^-}}{\frac{\phi_m^-}{M_m^-} - \frac{\phi_y^-}{M_y^-}} \quad (2.6)$$

Although the range of damage index in the three models is not uniform and different combinations used in calculating damage (the first two models are based on the combination of deformation and energy, and only deformation is considered in the third), all define the damage index for unity as the failure of global structure or local components. They can be applied to describe the damage for reinforced concrete sections. By the three damage models, the uncertainty of failure model caused by different damage models under same seismic load can be eliminated.

## 2.4 Global Structural Damage Model

The above-mentioned structural damage models mainly focus on local damage. However, local failure in structures caused by strong ground motion does not always lead to their global collapse which depends on both distribution and severity of the local damage. Generally, two aspects are considered in the evaluation of global structural damage, i.e. 1) The structure is treated as a whole, i.e. a large reaction system, and damage variable is defined by the variation of the overall mechanical properties before and after an earthquake, then evaluate seismic resistant behavior of structure; 2). The damage of each structural member is calculated and analyzed by local damage model, and the globe damage index can be expressed as the sum of the local damage by certain weight coefficient. The most widely used is a weighted combination method proposed by Park et al (Park et al., 1985), it can be defined as:

$$D = \sum \lambda_i D_i \quad (2.7)$$

in which  $\lambda_i = E_i / \sum E_i$ ,  $i$  = the first  $i$  member or story.  $E_i$  is the energy absorbed at member or story  $i$ .

The paper adopts this weighted combination method to evaluate the global structural damage, and the larger damage index between the initial and last section is treated as the damage index of the member, when the globe damage index for 1 indicates the global structural collapse. The computational process of the globe damage index sees Fig. 2.3.

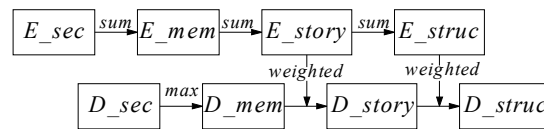


**Figure 2.3.** Computational process of the global damage index

## 3. SELECTION OF GROUND MOTION BASED ON RESPONSE SPECTRUM

Failure modes of structures would vary significantly with ground motions. It is unrealistic and unnecessary to obtain the optimal failure mode through inputting a large number of ground motions. Hence, how to find out the failure mode of maximum probability from limited ground motion is the key point, it requires that the discreteness of the failure modes under different ground motions can

reach minimum as much as possible. According to the selection of waves proposed by Yang et al (Yang et al., 2000), i.e. two frequency range of normal design response spectrum, firstly, from 0.1 to  $T_g$ ; secondly, from  $[T_1-\Delta T_1]$  to  $[T_1+\Delta T_2]$ , where  $\Delta T_1=0.2\text{sec}$ ,  $\Delta T_2=0.5\text{sec}$ , and  $T_1$  is structural basic period,  $T_g$  is site characteristic period (see Fig. 3.1). It requires that the difference is not more than 10% between the average of selected waves and normal design. By this selection, when inputting small ground motions, the discreteness of time-history analysis results can attain minimum (Yang et al, 2000).

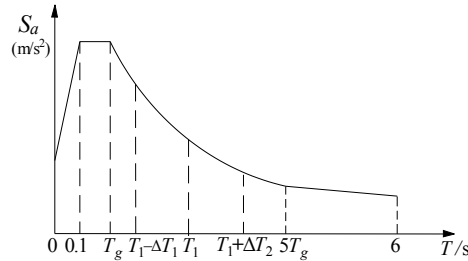


**Figure 3.1.** Frequency range of normal design response spectrum

In order to contrast, the normal design response spectrum is treated as target spectrum, then an artificial ground motion is synthesized based on the trigonometric series method, the acceleration time history and response spectrum of the artificial ground motion are shown in Figs. 3.2 and 3.3.

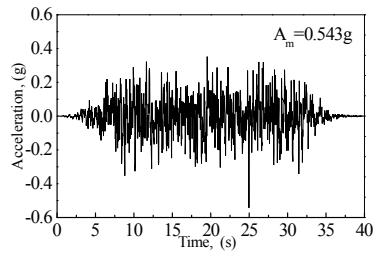


**Figure 3.2.** Acceleration time history

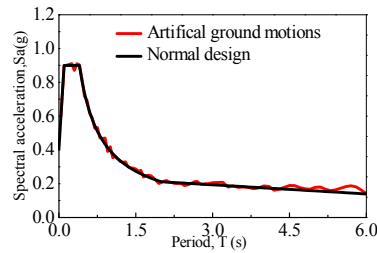


**Figure 3.3.** Response spectra

#### 4. FAILURE MODE OF MAXIMUM PROBABILITY BASED ON PCA MEHTOD

Considering the variation in structural responses caused by different ground motions, structural failure modes are therefore greatly different. The following two questions may be arise, i.e. 1) How to consider the influence of interrelationship between different ground motions on the sequence of failed sections of interest? 2) The times of failed sections occur in all cases of ground motions is different.

How to solve the above two questions is the key to search structural failure mode of maximum probability. Three methods are investigated in this paper for solving the problem, i.e., 1) The weighted average method combines the occurred number and sequence of one failed section under different ground motions; 2) The average size of  $S_a$  corresponding failed sections under different ground motions; 3) The principal component analysis (PCA) method in the statistics. Although the former two methods can be applied to evaluate, to some extent, the sequence of failed sections of interest, they cannot well consider interrelationship between different ground motions. In the application of the PCA method, the value of  $S_a$  corresponding to each failed section caused by different ground motions is treated as a variable and then failure sequence of all failed sections are determined by principal component scores. Therefore, the interrelationship between failure sequence determined by PCA and different ground motion becomes weakened. Basic principle and steps of PCA method are as follows:

##### 4.1 Basic Principle

PCA is a mathematical method on data dimension reduction. In many cases, when analyzing mutilate subjects by the statistical method, the variables have a certain correlation each other, namely that there is some overlap when the two variables reflect the subject at the same time. PCA means that some new variables can be proposed as small as possible based on the original, but these new variables are non-correlative each other, and can reflect the original information as much as possible.

## 4.2 Basic Steps

The PCA method can be briefly summarized as five steps, i.e. 1) Normalization of original data; 2) formation of a variable sample correlation coefficient matrix; 3) Solution of the characteristic roots of the matrix and corresponding the eigenvectors; 4) Calculation of the number of principal components according to cumulative variance contribution rate (generally above 85%); 5) Determination of the total score of principal components and their rankings.

## 5. EXAMPLE

According to *code for design of concrete structures* (GB50010, 2010) and *code for seismic design of buildings* (GB50011, 2010), a four-storey and three-bay reinforced concrete frame is established, the planar dimension of structure is shown in Fig. 5.1. The basic information for seismic design of the structure is: 1) 8 degree seismic fortification intensity; 2) 1st design earthquake group; 3) II-type site characteristic, and 4) site characteristic period  $T_g=0.40\text{sec}$ . Floor live load is  $2.0\text{kN/m}^2$  and dead load is  $6.0\text{kN/m}^2$ . Roofing live load is  $0.7\text{kN/m}^2$ , and dead load is  $7.5\text{kN/m}^2$ . The concrete beams, columns and boards adopt C40, longitudinal carrying bard adopt HRB400, and stirrups adopt HPB235, slab thickness 110mm, structural basic period  $T_1=0.96\text{sec}$ . According to structural layout rule, one planner frame can be modeled based on platform OpenSees. The serial numbers of sections see Fig. 5.2.

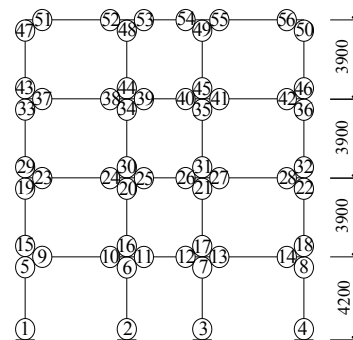
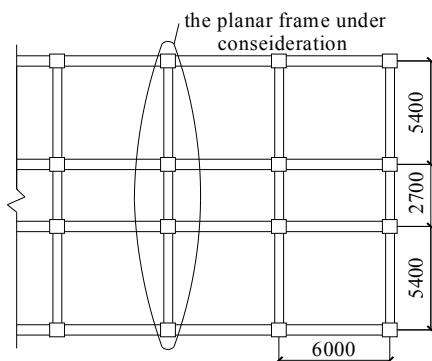


**Figure 5.1.** Planar dimension of the frame structure (mm)      **Figure 5.2.** Serial numbers of member sections

According to the Ref. (Yang et al., 2000), 14 natural ground motions are selected, all ground motion parameters are lined in Table 5.1. The acceleration response spectrum and average response spectrum see Figs. 5.3 and 5.4.

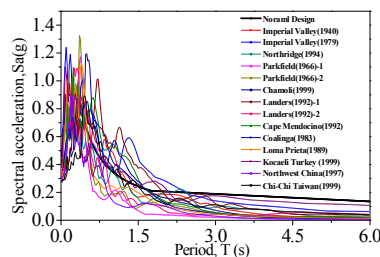


**Figure 5.3.** Acceleration response spectra

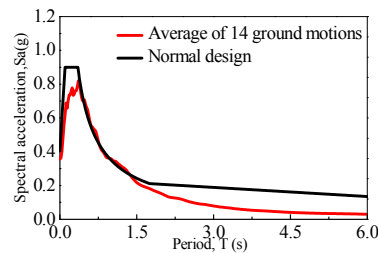


**Figure 5.4.** Average response spectra

**Table 5.1.** 14 Ground Motion Parameters

| No | M   | Earthquake             | Satation                         | Record/Component  | PGA (g) |
|----|-----|------------------------|----------------------------------|-------------------|---------|
| 1  | 7.0 | Imperial Valley(1940)  | 117 EI Centro Array#9            | IMPVALL/I-ELC180  | 0.313   |
| 2  | 6.6 | Imperial Valley(1979)  | 958 EI Centro Array #8           | IMPVALL/H-E08140  | 0.602   |
| 3  | 6.7 | Northridge(1994)       | 90009N.Hollywood-ColdwaterCan    | NORTHR/CWC270     | 0.277   |
| 4  | 6.1 | Parkfield(1966)-1      | 1438 Temblor pre-1969            | PARKF/TMB205      | 0.357   |
| 5  | 6.1 | Parkfield(1966)-2      | 1014 Cholame #5                  | PARKF/C05085      | 0.442   |
| 6  | 6.6 | Chamoli(1999)          | Gopeshwar,India                  | CHAMOLI/20        | 0.353   |
| 7  | 7.3 | Landers(1992)-1        | 22170 Joshua Tree                | LANDERS/JOS090    | 0.284   |
| 8  | 7.3 | Landers(1992)-2        | 23 Coolwater                     | LANDERS/CLW-LN    | 0.283   |
| 9  | 7.1 | Cape Mendocino(1992)   | 89324RioDellOverpass-FF          | CAPEMEND/RIO270   | 0.385   |
| 10 | 6.7 | Coalinga(1983)         | 1162 Pleasant Valley P.P. - bldg | COALINGA/H-PVP045 | 0.380   |
| 11 | 6.9 | Loma Prieta(1989)      | 47006 Gilroy - GavilanColl       | LOMAP/GIL067      | 0.357   |
| 12 | 7.5 | Kocaeli Turkey (1999)  | Sakarya                          | KOCAELI/SKR090    | 0.376   |
| 13 | 6.1 | Northwest China( 1997) | 19001                            | JIA CHINA/UP      | 0.277   |
| 14 | 7.6 | Chi-Chi Taiwan(1999)   | CHY029                           | CHICHI/CHY029-W   | 0.300   |

Based on the platform OpenSees, incremental dynamic analysis (IDA) with an increment of  $\Delta S_a=10\text{cm/s}^2$  is then performed to evaluate the positions of failed sections and the corresponding values of  $S_a$ , until global seismic damage exceeds 1.0. Global damage index and spectrum acceleration see Fig. 5.5. Failed sections and corresponding spectral acceleration see Fig. 5.6. Due to the limited space only six ground motions including an artificial ground motion are listed, others are similar.

As Fig. 5.5 shows, by three damage models, the structural damage degree under same ground motion is different, but the trend of global structural damage is uniform. It can be seen from Fig.12 that the failure modes obtained by three damage models under same ground motion are largely uniform, only corresponding the value of  $S_a$  is slightly different, and some sections have occurred failure or no failure by three damage models when the globe damage index is close to 1, such as the section ⑰ (see Fig. 5.6(e)).

Therefore, only the failed sections by three damage models at same ground motion are considered. For each ground motion, the average value of  $S_a$  by three damage models is treated as the failed  $S_a$  of each section. Failed  $S_a$  and corresponding section under all ground motions as listed in Table 5.2.

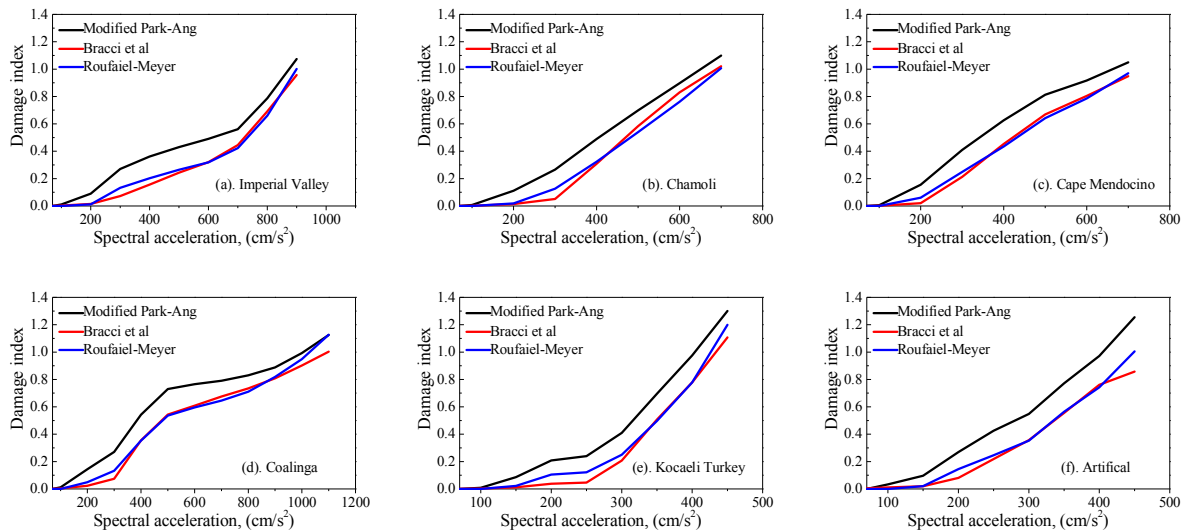


**Figure 5.5.** Global damage index vs. spectrum acceleration

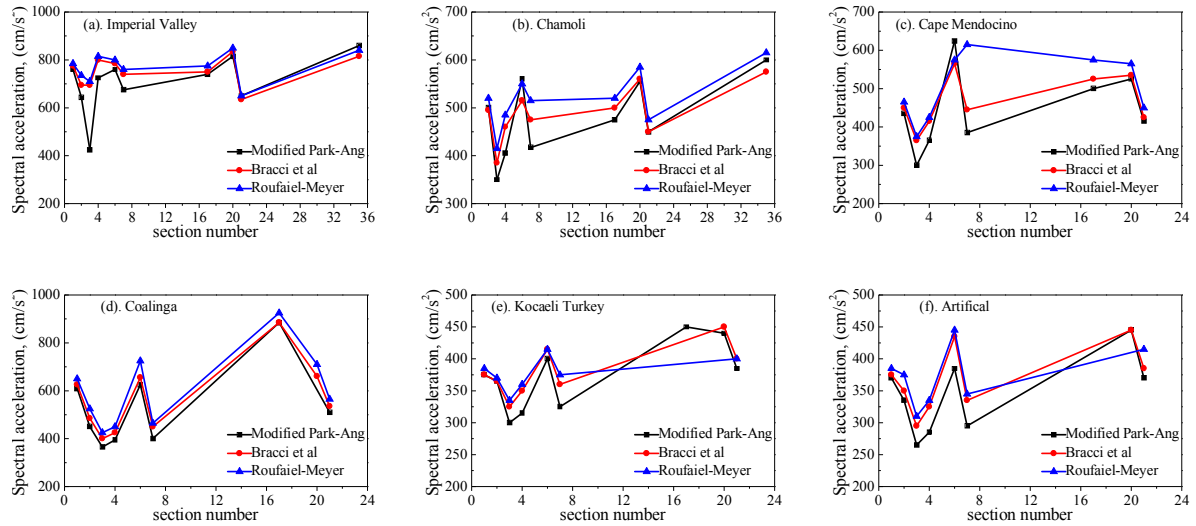


**Figure 5.6.** Failed sections and corresponding spectral acceleration

**Table 5.2.** Failed  $S_a$  ( $\text{cm/s}^2$ ) and Corresponding Section Under All Ground Motions

| Section | 1   | 2   | 3   | 4   | 5   | 6   | 7   | 8   | 9   | 10  | 11  | 12  | 13  | 14  | 15  |
|---------|-----|-----|-----|-----|-----|-----|-----|-----|-----|-----|-----|-----|-----|-----|-----|
| ①       | 773 | 336 | 628 | 460 | 428 | —   | 500 | 668 | —   | 628 | 383 | 378 | 565 | 410 | 377 |
| ②       | 692 | 293 | 593 | 387 | 505 | 452 | 500 | 450 | 487 | 325 | 367 | 402 | 543 | 387 | 353 |
| ③       | 610 | 230 | 537 | 383 | 395 | 383 | 367 | 397 | 347 | 397 | 258 | 320 | 542 | 345 | 290 |
| ④       | 780 | 267 | 650 | 508 | 450 | 502 | 478 | 402 | 423 | 280 | 342 | 427 | 578 | 362 | 315 |
| ⑥       | 782 | 382 | 657 | 657 | 542 | 545 | 517 | 587 | 668 | 337 | 410 | 446 | 575 | 413 | 422 |
| ⑦       | 725 | 316 | 618 | 458 | 469 | 483 | 488 | 482 | 438 | 297 | 353 | 407 | 556 | 385 | 325 |
| ⑰       | —   | —   | —   | 790 | 498 | —   | 600 | 523 | 533 | 898 | —   | —   | —   | —   | —   |
| ⑳       | 833 | 343 | 713 | 688 | 493 | 567 | 553 | 555 | 542 | 678 | —   | 445 | 592 | —   | 445 |
| ㉑       | 645 | 240 | 625 | 468 | 458 | 458 | 475 | 430 | 537 | 437 | 395 | 433 | 552 | 380 | 377 |
| ㉓       | 838 | —   | —   | —   | —   | 597 | —   | 650 | —   | —   | —   | —   | —   | —   | —   |

According to the size of failed  $S_a$  of each section, the failure modes under all ground motions can be obtained as listed in Table 5.3. It is obvious that the position of initial failed section under all ground motions is ③, and the occurred number of the sections ① ⑰ ⑳ ㉓ is less than 15 times, the section ㉓ only three times. It can be known that the failure probability of the section ㉓ is very small, and it is reasonable to ignore the section ㉓.

Therefore, first, the value of failed  $S_a$  corresponding the sections ② ④ ⑥ ⑦ ㉑ which occurred 14 times are analyzed by PCA based on the multivariate statistical analysis software SPSS. As Table 5.4 shows, P1, P2, P3 are principal components, and the failure sequence of sections is ④ → ⑦ → ② → ㉑ → ⑥. Second, due to the section ① occurred 12 times, and all failed sections ③ ④ ⑦ ② are prior to the section ① from Table 5.3. Then only considering the failed sequence among sections ① ㉑ ⑥, by similar method, the value of failed  $S_a$  corresponding the sections ① ㉑ ⑥ are analyzed by PCA again, and the final sequence is ㉑ → ① → ⑥. For the sequence of sections ⑥ ㉑ ⑰, it is obvious that the probability of failure sequence ⑥ → ㉑ → ⑰ is the largest from Table 5.3

In order to compare the results, the first 5 and last 9 ground motions are respectively analyzed by PCA method. The final results are shown in Table 5.5. P1, P2, P3 are principal components. The failure sequence of sections is ④ → ⑦ → ② → ⑥ → ㉑ by the first 5 ground motions and ④ → ㉑ → ⑦ → ② → ⑥ by the last 9 ground motions. It can be known that the discreteness of above three groups of failure sequence is small.

**Table 5.3.** Failure Modes of All Ground Motions

| No | Sequence               |   |   |   |   |   |   |   |   |   |
|----|------------------------|---|---|---|---|---|---|---|---|---|
|    | Ground motion          | 1 | 2 | 3 | 4 | 5 | 6 | 7 | 8 | 9 |
| 1  | Imperial Valley (1940) | ③ | ② | ② | ⑦ | ① | ④ | ⑥ | ⑩ | ⑤ |
| 2  | Imperial Valley (1979) | ③ | ② | ④ | ② | ⑦ | ① | ⑩ | ⑥ |   |
| 3  | Northridge(1994)       | ③ | ② | ⑦ | ② | ① | ④ | ⑥ |   |   |
| 4  | Parkfield(1966)-1      | ③ | ② | ⑦ | ① | ② | ④ | ⑥ | ⑩ | ⑦ |
| 5  | Parkfield(1966)-2      | ③ | ② | ⑦ | ④ | ① | ② | ⑥ | ⑩ | ⑦ |
| 6  | Chamoli(1999)          | ③ | ④ | ② | ② | ② | ⑥ | ⑩ | ⑤ |   |
| 7  | Landers (1992)-1       | ③ | ② | ② | ② | ① | ④ | ⑥ | ⑩ | ⑦ |
| 8  | Landers (1992)-2       | ③ | ② | ④ | ② | ② | ⑥ | ⑦ | ⑩ | ① |
| 9  | Cape Mendocino(1992)   | ③ | ④ | ② | ② | ⑦ | ⑦ | ⑩ | ⑥ |   |
| 10 | Coalinga(1983)         | ③ | ④ | ⑦ | ② | ② | ① | ⑥ | ⑩ | ⑦ |
| 11 | Loma Prieta(1989)      | ③ | ④ | ⑦ | ② | ⑥ | ① | ② |   |   |
| 12 | Kocaeli Turkey(1999)   | ③ | ④ | ⑦ | ② | ① | ② | ⑥ | ⑩ |   |
| 13 | Chi-Chi Taiwan(1999)   | ③ | ② | ② | ⑦ | ① | ⑥ | ④ | ⑩ |   |
| 14 | Northwest China(1997)  | ③ | ④ | ② | ⑦ | ② | ① | ⑥ |   |   |
| 15 | Artificial             | ③ | ④ | ⑦ | ② | ① | ② | ⑥ | ⑩ |   |

**Table 5.4.** PCA Results of 14 Ground Motions

| Section | P1     | P2     | P3     | Total  | Rank            |
|---------|--------|--------|--------|--------|-----------------|
| ②       | -1.576 | 1.631  | -1.543 | -1.489 | 3 <sup>rd</sup> |
| ④       | -0.988 | -3.001 | 0.378  | -3.611 | 1 <sup>st</sup> |
| ⑥       | 5.031  | 0.280  | 0.042  | 5.353  | 5 <sup>th</sup> |
| ⑦       | -0.951 | -0.317 | -1.200 | -2.470 | 2 <sup>nd</sup> |
| ⑩       | -1.514 | 1.408  | 2.323  | 2.217  | 4 <sup>th</sup> |

**Table 5.5.** PCA Results of First 5 Ground Motions

| Section | P1     | P2     | P3     | Total  | Rank            |
|---------|--------|--------|--------|--------|-----------------|
| ②       | -1.246 | 1.394  | -0.321 | -0.173 | 4 <sup>th</sup> |
| ④       | 0.2157 | -1.557 | -0.535 | -1.876 | 1 <sup>st</sup> |
| ⑥       | 2.991  | 0.469  | 0.334  | 3.796  | 5 <sup>th</sup> |
| ⑦       | -0.372 | 0.155  | -0.435 | -0.652 | 3 <sup>rd</sup> |
| ⑩       | -1.588 | -0.463 | 0.957  | -1.094 | 2 <sup>nd</sup> |

**Table 5.5.** PCA Results of Last 9 Ground Motions

| Section | P1     | P2     | P3     | Total  | Rank            |
|---------|--------|--------|--------|--------|-----------------|
| ②       | -0.997 | -0.201 | -0.248 | -1.447 | 3 <sup>rd</sup> |
| ④       | -1.636 | -1.415 | -1.795 | -4.847 | 1 <sup>st</sup> |
| ⑥       | 3.962  | -0.610 | -0.790 | 2.561  | 4 <sup>th</sup> |
| ⑦       | -1.024 | -0.702 | -0.883 | -2.610 | 2 <sup>nd</sup> |
| ⑩       | -0.304 | 2.929  | 3.719  | 6.344  | 5 <sup>th</sup> |

Finally, the structural failure mode of maximum probability is ③ → ④ → ⑦ → ② → ⑩ → ① → ⑥ → ⑩ → ⑦, but the failure mode based on the artificial ground motion is ③ → ④ → ⑦ → ② → ① → ⑩ → ⑥ → ⑩. The two groups of failure mode are very close. From above results, it can be drawn that the discreteness of the failure mode under different ground motions can be controlled based on normal design response spectrum, and the failure mode of maximum probability can be predicted by PCA.

## 6. CONCLUSIONS

The paper considered the variation caused by different ground motions on structural responses, and

obtained the structural failure mode of maximum probability by combining structural damage model and PCA in the mathematical statistics. Results show that: 1). By three damage models, the structural damage degree under the same ground motion is different, but the trend of global structural damage is uniform. 2). The failure modes obtained by three damage models under same ground motion is largely uniform. Under the discreteness of different ground motions on normal design minimization premise: the position of initial failed section under different ground motions is same. 3) The discrete structural failure modes under different ground motions can be very well controlled based on normal design. It is feasible that the failure mode of maximum probability can be predicted by PCA method.

#### ACKNOWLEDGEMENT

This research was financially supported by the National Natural Science Foundation of China (Grant No. 90915005 and 51161120359), the Program for New Century Excellent Talents in University (NCET) of the Ministry of Education of China (Grant No. NCET-08-0096) and the National Key Technologies R&D Program of China (Grant No. 2009BAJ28B03).

#### REFERENCES

- Bai, J.L., and Ou, J.P. (2011). Optimization of failure modes for reinforced concrete buildings based on IDA method. *ENGINEERING MECHANICS* 28:S2,198-203. (in Chinese).
- Banon, H., Lrvine, H.M. and Biggs, J.M. (1987). Seismic damage in reinforced concrete frames. *Journal of Structural Engineering* 107:9,1713-1729.
- Bracci, J.M., Mander, J.B. and Kunnath, S.K. (1989). Deterministic model for seismic damage evaluation of RC structures. *Technical Report NCEERR-89-0033*. National Center for Earthquake Engineering Research, Buffalo, New York, USA.
- Feng, Y.S. (1988). Enumerating significant failure modes of a structural system by using criterion methods. *Computes & Structures* 30:3,1153-1157. (in Chinese).
- Gharaibeh, E.S., Frangopol, D.M. and Onoufriou, T. (2002). Reliability based importance assessment of structural members with applications to complex structures. *Computes & Structures* 80:12,1113-1131.
- Hou, G.L. (2001). Structural reliability indicators, the probability vector, pushover analysis and system reliability. Harbin Institute of Technology, Harbin, China. (in Chinese).
- Kunnath, S.K., Reinhorn, A.M. and Abel, J.F. (1992). A computational tool for seismic performance of reinforced concrete buildings. *Computers & Structures* 41:1,157-173.
- Melchers, R.E. and Tang, T.K. (1984). Dominant failure modes in stochastic structural systems. *Structural Safety* 2:2,127-143.
- Moses F. (1982). System reliability development in structural engineering. *Structural Safety* 26:1,3-13.
- Murotsu, Y. et al. (1984). Automatic generation of stochastically dominant modes of structural failure in frame structure. *Structural Safety* 28: 2,17-25.
- Ou, J.P. and Duan, Y.B. (1995). Seismic reliability analysis and optimum design of tall buildings. *Earthquake Engineering & Engineering Vibration* 15:1,1-13. (in Chinese).
- Park, Y.J., Ang, A.H-S. and Wen, Y.K. (1985). Seismic damage model for reinforced concrete. *Journal of Structural Engineering* 111:4,740-757.
- Park, Y.J., Ang, A.H-S. (1985). Mechanistic seismic damage model for reinforced concrete. *Journal of Structural Engineering* 111:4,722-739.
- Park, Y.J., Ang, A.H-S. and Wen, Y.K. (1987). Damage - limiting aseismic design of buildings. *Earthquake Spectra* 3:1,1-26
- Park, S., Choi, S. and Sikorsky, C. et al. (2004). Efficient method for calculation of system reliability of a complex structure. *International Journal of Solids and Structures* 41:18-19,5035-5050.
- Roufaiel, M.S.L. and Meyer, C. (1987). Analytical modeling of hysteretic behavior of R/C frames. *Journal of Structural Division* 113: 3,429-444.
- Thoft-Chistensen, P. and Murotsu, Y. (1986). Application of Structural Systems Reliability Theory, Springer-Verlag, New York. U.S.A.
- Yang, F., Li, Y.M. and Lai, M. (2000). A new method for selecting inputting waves for time-history analysis. *China Civil Engineering Journal* 33: 6,34-37. (in Chinese).
- Yao, W.X. and Gu, Y. (1996). Numerating significant failure modes of a structural system by using automatic matrix force method. *Computational Structural Mechanics and Applications* 13:1 63-66. (in Chinese).